

## TWO-PHASE FLOW THROUGH A STAGGERED TUBE BUNDLE OF A SHELL AND TUBE HEAT EXCHANGER

Sadikin A.<sup>1\*</sup> and McNeil D.A.<sup>2</sup>

\*Author for correspondence

<sup>1</sup> Faculty of Mechanical Engineering and Manufacturing,  
Universiti Tun Hussein Onn Malaysia,  
86400 Parit Raja, Batu Pahat, Johor,  
Malaysia,

<sup>2</sup> School of Engineering and Physical Sciences,  
Heriot-Watt University,  
EH14 4AS,  
United Kingdom,

\*E-mail: azmah@uthm.edu.my

### ABSTRACT

Two-phase flow on the shell side of a shell and tube heat exchanger is complex. This paper contributes to the existing data base by presenting data for void fraction and pressure drops for tubes with a diameter of 19 mm. Results for air-water flows near atmospheric pressure are presented. The results were obtained for flows through a column of a thin-slice, staggered tube bundle containing 22 rows. It contained four full columns of tubes and two columns of half tubes placed on the shell walls. The tubes were 19 mm in diameter and 50 mm long with a pitch to diameter ratio of 1.32 and were arranged in a staggered triangular configuration. Previous studies have shown that the void fraction in a shell-side, gas-liquid flow becomes constant after only a few rows. Thus, the void fraction was only measured at one location. A gamma-ray densitometer was used to measure the void fractions. Corresponding pressure drops were obtained between rows 3 and 15. Data are presented for a mass flux range of 25-688 kg/m<sup>2</sup>s and a gas mass fraction range of 0.0005-0.6. The measurements are shown to compare reasonably well with correlations available in the open literature.

### INTRODUCTION

Shell and tube heat exchangers are widely used in the process industry for boiling applications. The design of these units is usually based on a one-dimensional formulation of the flowing fluid. This approach requires knowledge of the void fraction and the two-phase multiplier. For shell-side boiling, several investigators have proposed void fraction correlations [1,2,3] while [4,5] have proposed commonly used two-phase multiplier correlations. The void fraction correlation [1] was derived from data obtained using air-water in tube bundles

containing tubes 7.94 mm in diameter. The void fraction correlation [2] was derived from data obtained using air-water in tube bundles containing tubes 12.7 mm and 19.05 mm in diameter. The void fraction correlation [3] was derived from data obtained using R11 in tube bundles containing tubes 6.35 mm in diameter.

### NOMENCLATURE

$Ca$	[-]	Capillary number
$D$	[m]	Tube diameter
$Fr$	[-]	Froude number
$g$	[m <sup>2</sup> /s]	Gravity acceleration
$I_B$	[-]	Background readings
$I_L$	[-]	The water-only gamma-ray intensity
$I_G$	[-]	The air-only gamma-ray intensity
$I$	[-]	Two-phase mixture gamma-ray intensity
$j_G$	[m/s]	Superficial velocity
$j_G^*$	[m/s]	Dimensionless gas velocity
$k$	[-]	Slip ratio
$m$	[kg/m <sup>2</sup> s]	Mass flux
$P$	[m]	Tube pitch
$Ri$	[-]	Richardson number
$u_G$	[m <sup>2</sup> /s]	Gas velocity
$v_G$	[m <sup>3</sup> /kg]	Specific volume of the gas
$v_L$	[m <sup>3</sup> /kg]	Specific volume of the liquid
$x$	[m]	Quality
$X_{TT}$	[-]	Martinelli parameter
Special characters		
$\alpha$	[-]	Void fraction
$\alpha_H$	[-]	Homogenous void fraction
$\rho$	[kg/m <sup>3</sup> ]	Density
$\rho_G$	[kg/m <sup>3</sup> ]	Density of the gas
$\rho_L$	[kg/m <sup>3</sup> ]	Density of the liquid
$\rho_{TP}$	[kg/m <sup>3</sup> ]	Two-phase density
$\mu_L$	[kg/m.s]	Dynamic viscosity of the liquid
$\phi_L^2$	[-]	Two-phase frictional multiplier

Subscripts

A	Acceleration
F	Frictional
G	Gravitational

The friction pressure drop correlation [4] was derived from data obtained using several fluids and tube bundles. The purpose of this study is to obtain void fraction and pressure drop data for air-water flows near atmospheric pressure and temperature for a tube bundle containing tubes 19 mm in diameter and to test these against existing correlations for void fraction and two-phase multiplier.

## EXPERIMENTAL APPARATUS

The flow loop used to obtain the experimental data is illustrated in Figure 1. The water was taken from the supply tank and driven by a positive displacement pump. The water flow from the pump could either flow to the test section or be returned to the supply tank via the re-circulation line. The required water flow rate was achieved by adjusting the manual valve placed in the recirculation line. The water entered the test section after passing through one of four parallel flow nozzles used to measure the water flow rate. Each nozzle had a different throat diameter, allowing a wide range to be measured. The accuracy of the water flow measurements was  $\pm 1.0\%$ .

Compressed air flowed from the supply vessel to one of two Fisher-Rosemount-Brooks rotameters, before entering the test section through two porous tubes placed in the bubble generator. A gate valve downstream of each magnetically coupled rotameter allowed the air flow rate to be adjusted. The two parallel flow meters had ranges of 0-0.0039 and 0-0.034 kg/s. The flow meters were calibrated for the line pressure and were accurate to  $\pm 1.6\%$  of reading.

The two-phase mixture flowed up through the test section and into the air-water separator, from which the air was discharged to the atmosphere and the water returned to the supply tank.

The bubble generator contained two pieces of porous tube (SIKA-B) manufactured by GKN Sinter Metals. They were 110 mm long and 50.0 mm in outside diameter and they had an effective pore size of 206 microns. They were placed in a rectangular Perspex box 224 mm in height  $\times$  100 mm in depth  $\times$  100 mm in width. Water entered the Perspex box from below. The air was fed to the porous tubes from both sides to produce a reasonably even two-phase flow that passed through the first convergent section and the 244 mm settling length before entering the tube bundle. A further convergent section connected the test section to the pipe linked to the air-water separator.

The tube bundle contained ten rows of tubes with an outside diameter of 19.0 mm. It contained four full columns of tubes and two columns of half tubes placed on the shell walls to reduce bypass leakage. The tubes were 56.0 mm in length, with 50 mm exposed to the fluid. The remaining 6.0 mm was inserted into 3 mm grooves that were milled using a CNC mill

on the front and rear tube sheets. The tubes were arranged in staggered configuration with a pitch to diameter ratio of 1.32.

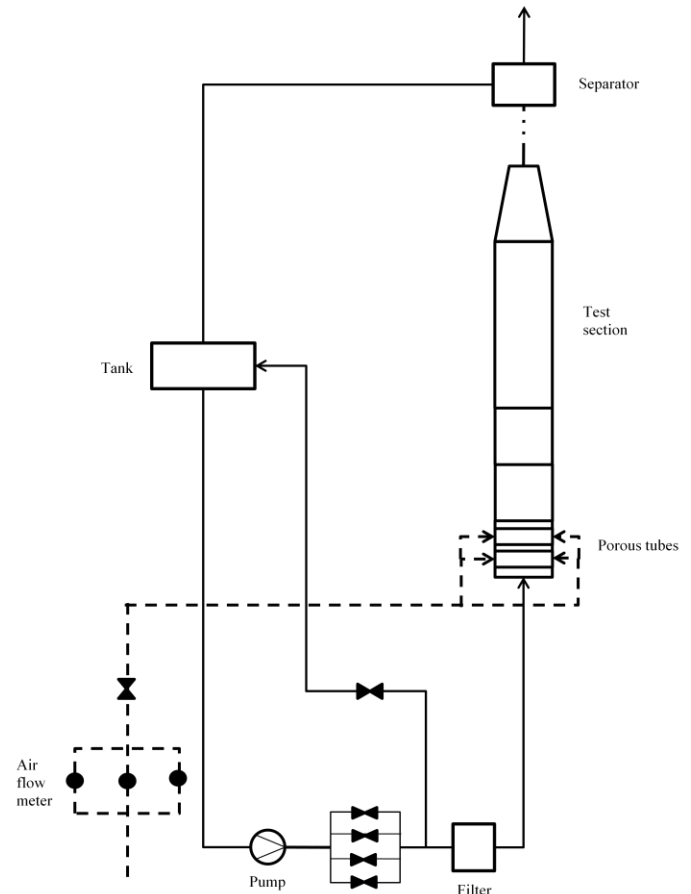
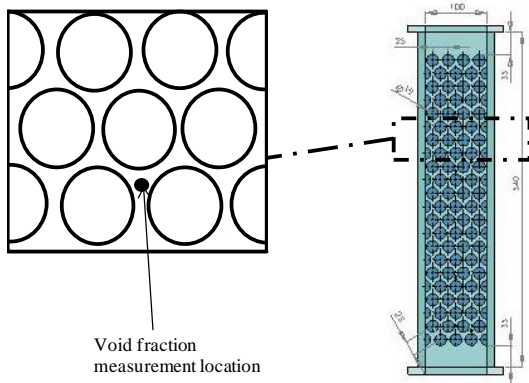


Figure 1 In-bundle flow loop

The material for the sheets and tubes was Perspex which give a clear view of the flow. Two pressure taps were used in this study, one located mid-way between rows 2 and 3 and one mid-way between rows 14 and 15. These allowed pressure drops across eleven tubes to be measured. The first two and the last rows were excluded to avoid entrance and exit effects. The pressure drops were measured using a smart pressure transducer, accurate to 0.25% of range, which allowed the pressure drop range to be adjusted. The upper range value was set to accommodate the expected pressure drop and thus maximize the accuracy of the measurement. The fluid pressure was measured at the lower pressure tap by a gauge pressure transmitter accurate to 0.25% of range. The temperature of the two-phase mixture was measured by a K-type thermocouple located on the pipe between the test section and the separator. Temperatures were measured to an accuracy of  $\pm 0.5$  K.

Void fraction measurements were made using a gamma-ray densitometer at the maximum gap to the south of the central tube as shown in Figure 2. The densitometer isotope was Americium (Am) 241. This collimated low-energy source projected a beam 10 mm in diameter through the flow, parallel to the tubes, onto a photomultiplier tube. A PC card-based

electronically controlled pulse counter was used to measure the incident radiation.



**Figure 2** Test section and void fraction measurement location

## EXPERIMENTAL DATA

Two test series were conducted. The first obtained the pressure-drop data and the others obtained void fraction measurement. Each data set was obtained at the same nominal conditions as previous work in [6]. Tests were performed for a fixed total mass flow rate, thus as the gas mass flow rate increased, the liquid mass flow rate decreased. At the lowest total mass flow rate, the gas mass flow rate varied from 0.00039-0.017 kg/s while the liquid mass flow rate varied from 0.03-0.013 kg/s. At the highest total mass flow rate, the gas mass flow rate varied from 0.00039-0.027 kg/s while the liquid mass flow rate varied from 0.93-0.9 kg/s. Nine total mass flow rates were used for each data set, giving a gas mass fraction range of 0.00047-0.57 and a mass flux range, based on the minimum flow area between the tubes, of 25-688 kg/m<sup>2</sup>s.

Tests were conducted by setting the water flow rate to the required value before setting the air flow rate to its required value. The flow resistance in the test facility was dependent on these flow rates so that the exact conditions were achieved by making minor adjustments to each as appropriate. When the desired conditions were achieved, the mass flow rates and the pressure and temperature were measured. The air-flow rate was read manually. The water mass flow rate, the pressure and the temperature measurements were collected through a data logger connected to a PC controlled by LabVIEW software. Subsequent to this, depending on the data set undertaken, measurements of pressure drop or void fraction were taken.

### Pressure drop tests

Pressure-drop measurements were collected through a data logger connected to a PC and controlled by LabVIEW software. Before the pressure drop readings were taken, all sampling lines in the pressure-drop measurement system were purged with water to remove any resident air. The pressure

drop signal fluctuated significantly so that 10000 readings were taken at a rate of 1 kHz to ensure representative averages.

Figure 3 shows the measured pressure drop. At the lowest mass flux of 25 kg/m<sup>2</sup>s, the pressure drop continues to decrease as the gas mass fraction increases because the gravitational pressure drop is more significant than the frictional pressure drop. The total pressure drop trend is different at the higher mass fluxes, for instance at 416 kg/m<sup>2</sup>s, where the total pressure drop increases with increasing quality because the frictional pressure drop is increase always higher than gravitational pressure drop decrease.

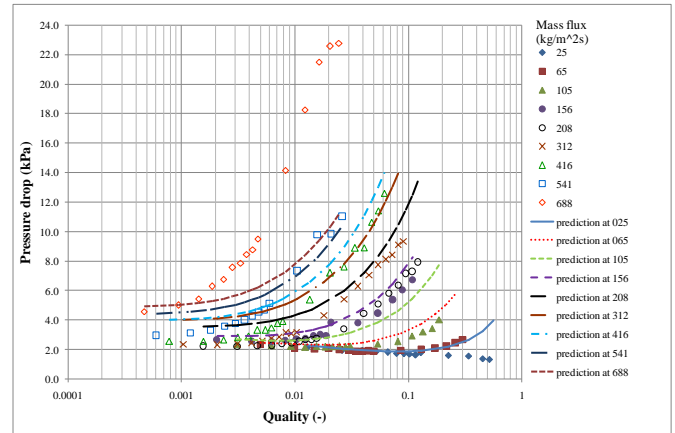


**Figure 3** Variation of measured pressure drop with quality and predicted pressure drop using predicted void fraction [2] for gravitational pressure drop and [5] frictional pressure drop

### Void fraction tests

Void fractions measurements were taken by aligning the single-beam, gamma ray densitometer in the gap to the south of the central tube. The tests were carried out at the nominal condition described in [6] and there were 290 data points of void fractions measurement. Prior to testing, the gamma-ray densitometer was set at the desired position relative to the central tube on row 16, i.e. the minimum gap to the east or the south. Before the Am241 source was installed, background readings,  $I_B$ , were taken. After the source was installed the air-only readings,  $I_G$ , were taken. After the water flow had been set, the water-only readings,  $I_L$ , were taken. The two-phase readings,  $I$ , were obtained after the test conditions had been set. All readings were obtained from the electronic counter within the PC via the densitometer's software. One hundred readings were taken over a period of 100 s so that a representative average of each was obtained. The void fraction,  $\alpha$ , is defined as the ratio of the flow area occupied by gas to the total flow area and was found from these measurements through [7]

$$\alpha = \frac{\ln(I - I_B) - \ln(I_L - I_B)}{\ln(I_G - I_B) - \ln(I_L - I_B)} \quad (1)$$

The void fraction variation with quality is shown for a range of mass fluxes in Figure 4.

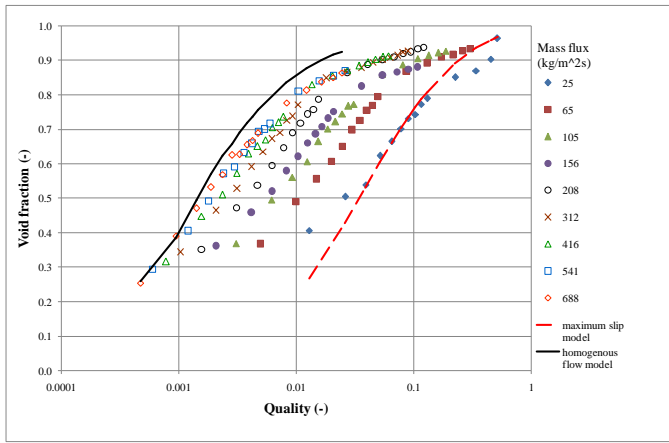


**Figure 4** Variation of measured void fraction with quality in the 19 mm staggered bundle

The void fraction is shown to increase with increasing gas-mass fraction, as would be expected. It is also shown to increase with increasing mass flux, again consistent with other findings [1,2,3]. Included in Figure 4 are the homogeneous and maximum slip models [8]. These void fractions were determined from

$$\alpha = \frac{xv_G}{(xv_G + k(1-x)v_L)} \quad (2)$$

in which  $x$  is the gas mass fraction and  $v_G$  and  $v_L$  are the specific volumes of the gas and liquid phases respectively. The slip ratio,  $k$ , depends on the model. The homogeneous model assumes that the gas and liquid phases travel at the same velocity, giving the slip ratio as unity. The maximum slip model assumes equal momentum flux in the gas and liquid streams of the separated flow model and is found from

$$k = \sqrt{\frac{v_G}{v_L}} \quad (3)$$

Void fraction data for one-dimensional flows are said to fall between the maximum slip and the homogeneous values. The current data are shown to be reasonably consistent with this view.

## DATA ANALYSIS

Two-phase pressure gradients,  $dp/dz$ , contain three components, the acceleration component,  $(dp/dz)_A$ , the gravitational component,  $(dp/dz)_G$ , and the frictional component,  $(dp/dz)_F$ , thus

$$\frac{dp}{dz} = \left(\frac{dp}{dz}\right)_A + \left(\frac{dp}{dz}\right)_G + \left(\frac{dp}{dz}\right)_F \quad (4)$$

In tube bundles only the latter two are important. The gravitational pressure gradient is

$$\left(\frac{dp}{dz}\right)_G = -\rho_{tp} g \quad (5)$$

where  $g$  is the acceleration due to gravity and  $\rho_{tp}$  is the two-phase density, which can be determined from

$$\rho_{tp} = \alpha \rho_G + (1-\alpha) \rho_L \quad (6)$$

in which  $\rho_G$  and  $\rho_L$  are the densities of the gas and liquid phases respectively.

## Void fraction comparisons

The measured void fractions were compared to three correlations [1,2,3]. [1] reported that the void fraction could be found from

$$\alpha = \alpha_H R \text{ where } R = \max(1 + 0.123 Fr^{-0.191} \ln x, 0.1) \quad (7)$$

where  $\alpha_H$  is homogenous void fraction found from equation (2) with a slip ratio of unity and  $Fr$  is the Froude number, defined through

$$Fr = \frac{m}{\rho_L \sqrt{gD}} \quad (8)$$

in which  $D$  is the tube diameter. The measured and predicted values are compared in Figure 5. The comparison is poor with most predictions outside the upper and lower limits set at  $\pm 30\%$ . This is consistent with other findings [2].

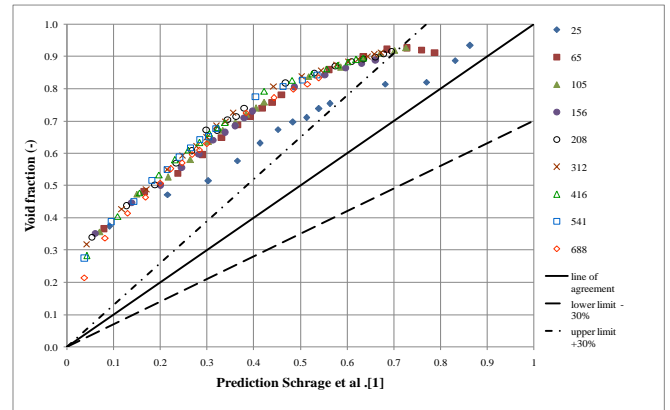


**Figure 5** Variation of measured and predicted void fraction [1]

The void fraction [2] could be found from

$$\alpha = 1 - \frac{1}{(1 + C_1 j_G^* + C_2 j_G^{*2})^{1/2}} \quad (9)$$

where  $j_G^*$  is the Wallis parameter, defined through

$$j_G^* = \frac{\sqrt{\rho_G} j_G}{\sqrt{gD(\rho_L - \rho_G)}} \quad (10)$$

and  $C_1$  and  $C_2$  depend on the fluid and the geometry of the tube bundle. For these data  $C_1 = 30$  and  $C_2 = 50$  were used, [9]. The superficial gas velocity,  $j_G$ , is evaluated in the minimum gap between the tubes through

$$j_G = xmv_G \quad (11)$$

The comparison between the measured values and the [2] predictions are shown in Figure 6. The comparison is reasonably good, with virtually all of the predictions within the upper and lower limits of  $\pm 30\%$ .

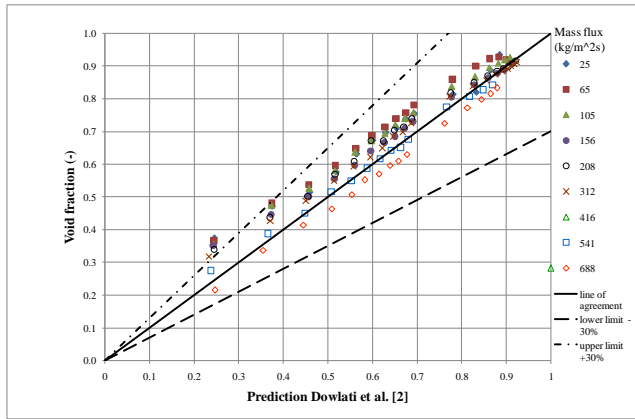


**Figure 6** Variation of measured and predicted void fraction [2]

[3] proposed a correlation for the slip ratio, allowing the void fraction to be determined from equation (2). The slip ratio was found from

$$k = 1 + 25.7 \frac{D}{P} \sqrt{Ri Ca} \quad (12)$$

where  $P$  is the tube pitch,  $Ca$  the capillary number and  $Ri$  the Richardson number. The Capillary number is defined as

$$Ca = \frac{\mu_L u_G}{\sigma} \quad (13)$$

where  $\mu_L$  is the dynamic viscosity of the liquid,  $\sigma$  is the surface tension and  $u_G$  the gas velocity in the minimum gap between the tubes, i.e.

$$u_G = \frac{xm}{\alpha \rho_G} \quad (14)$$

The Richardson number is defined through

$$Ri = \frac{(\rho_L - \rho_G)^2 g (P - D)}{m^2} \quad (15)$$

The comparison between the measured values and the [3] predictions are shown in Figure 7. The comparison is good, with a reasonable proportion of the predictions within the upper and lower limits of  $\pm 30\%$ .

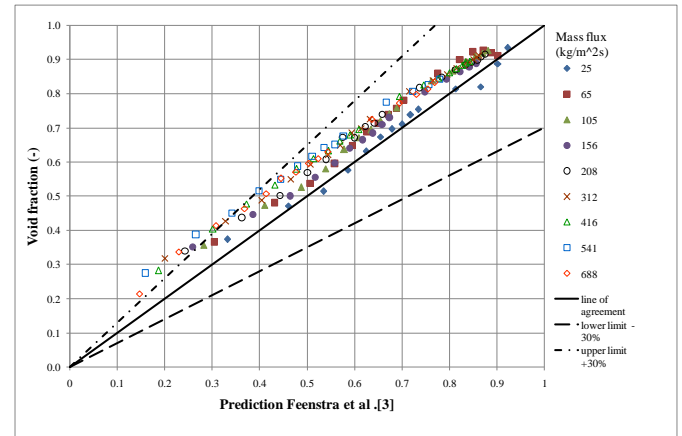


**Figure 7** Variation of measured and predicted void fraction [3]

### Two-phase multiplier comparisons

The two-phase multiplier,  $\phi_L^2$ , is related to the frictional pressure gradient through

$$\left( \frac{dp}{dz} \right)_F = \left( \frac{dp}{dz} \right)_L \phi_L^2 \quad (16)$$

where  $(dp/dz)_L$  is the single-phase frictional pressure gradient that would occur if the liquid portion of the flow passed through the heat exchanger. This was evaluated from [10]. The experimental gravitational pressure gradient was obtained from the measured void fraction, equations (5, 6). With the acceleration pressure gradient neglected, the experimental frictional pressure gradient was obtained by subtracting the measured gravitational value, from the measured value, Equation (4). The two-phase multiplier followed from equation (16).

A correlation for two-phase multiplier was reported by [4] as

$$\phi_L^2 = 1 + \frac{8}{X_{tt}} + \frac{1}{X_{tt}} \quad (17)$$

where  $X_H$  is the Martinelli parameter determined from

$$X_{tt} = \left( \frac{1-x}{x} \right)^{0.9} \sqrt{\frac{\rho_G}{\rho_L}} \left( \frac{\mu_L}{\mu_G} \right)^{0.1} \quad (18)$$

Figure 8 shows a comparison between the measured and predicted two-phase multiplier of [4] correlation, varying with Martinelli parameter. The measured values are deduced from the difference between the measured and gravitational pressure gradients. The measured two-phase multiplier clearly shows a mass flux dependency. At small quality, where the Martinelli parameter is large, the gravitational pressure drop is large in comparison to the frictional pressure drop and therefore similar in magnitude to the total pressure drop, potentially giving a significant error in the two-phase multiplier. At large quality, where the Martinelli parameter is small, the frictional pressure drop is more significant than the gravitational pressure drop, giving a small error. As the mass flux increases, the data moves towards the predicted values, with reasonable agreement for mass fluxes above 208 kg/m<sup>2</sup>s. This is said to be consistent with [2], where the correlation works well for mass flux greater than 260 kg/m<sup>2</sup>s. As seen from the graph, when the mass flux was 25 kg/m<sup>2</sup>s, a quality of 0.013 gave a Martinelli parameter of 2.66 and a gravitational pressure drop that was 93% of the total, while a quality of 0.52 gave a Martinelli parameter of 0.049 and a gravitational pressure drop that was 23% of the total. Similarly, when the mass flux was 688 kg/m<sup>2</sup>s, a quality of 0.00047 gave a Martinelli parameter of 57.8 and a gravitational pressure drop that was 44% of the total, while a quality of 0.025 gave a Martinelli parameter of 1.98 and a gravitational pressure drop that was 1.5% of the total.

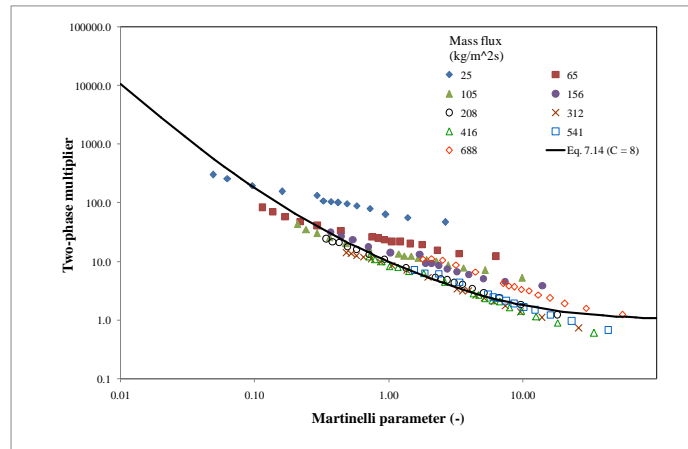


**Figure 8** Two-phase friction multiplier data with Martinelli parameter

A comparison between the measured two-phase multipliers and correlation of [4] is shown in Figure 9. At the lowest mass flux of 25 kg/m<sup>2</sup>s, the measured two-phase multiplier was considerably above the predicted value with an average difference of 317% and a RMS difference of 430%. As the mass flux increases, the data move towards the predicted

values, with reasonable agreement occurring for mass fluxes at 208 kg/m<sup>2</sup>s to 541 kg/m<sup>2</sup>s. At 541 kg/m<sup>2</sup>s, the mean error is -21% and RMS is 31%. This is consistent with previous studies, Dowlati et al. <sup>2</sup> where the correlation was said to be valid for mass fluxes greater than 260 kg/m<sup>2</sup>s. However, at the highest mass flux, 688 kg/m<sup>2</sup>s, the average and RMS differences were 85% and 94% respectively. The measured two-phase multipliers are greater than the predicted values and move upward from the agreement line.

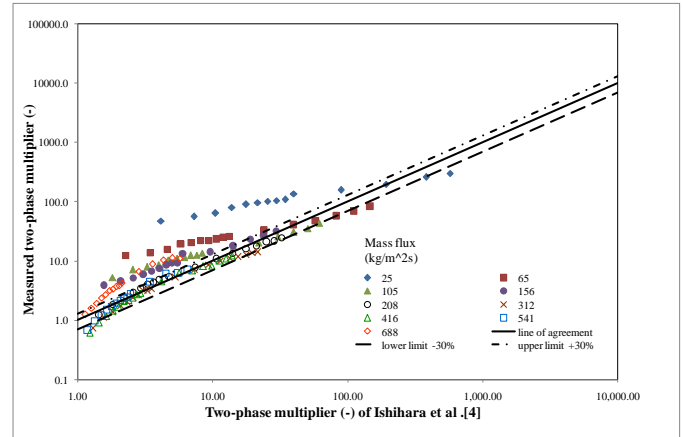


**Figure 9** Variation of measured with predicted two-phase multipliers of [4]

Figure 10 shows a comparison between the measured and predicted two-phase multipliers of [5]. The comparison gave better average and RMS differences than [4]. They fell from -5% to 37% at the lowest mass flux of 25 kg/m<sup>2</sup>s. At 541 kg/m<sup>2</sup>s, the mean average is 0.12% and the RMS error is 20%. A reasonable RMS difference of less than 40% is achieved for mass fluxes of 208 kg/m<sup>2</sup>s to 541 kg/m<sup>2</sup>s.

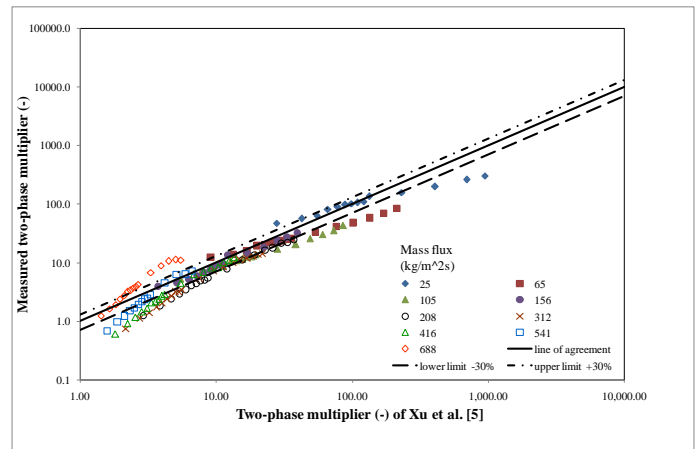


**Figure 10** Variation of measured with predicted two-phase multipliers of [5]

## DISCUSSION AND CONCLUSIONS

Of the three void fraction correlations compared to the measured data in Figures 5-7, the correlation of [2] is shown to represent the data best. It is therefore included in Figure 6, where it is shown to capture the data trends reasonably well. These data conform to the view that void fractions should be greater than those predicted from the maximum slip condition and less than those predicted from homogeneous flow. The [2] correlation clearly predicts values below the maximum slip values.

There are not that many methods available for shell-side flows and the correlation presented by [4] is clearly not universal. The best agreement with the measured two-phase multipliers was obtained with the [5] correlation. However, the comparison shows high mean average and RMS error at the highest mass flux, at 688 kg/m<sup>2</sup>s where the comparison gave 57% and 73% respectively.

The predicted pressure drop is best using using the [2] correlation for void fraction and the [5] correlation for frictional pressure gradient is compared with the measured data in Figure 3. The predictions do pick up the trends, e.g. the prediction at a mass flux of 25 kg/m<sup>2</sup>s is continually falling, in line with the data, while at the larger mass flux of 416 kg/m<sup>2</sup>s the turning characteristic is reproduced. However, the actual magnitudes are not well reproduced, as is typical of two-phase pressure drop predictions. The most of the data is predicted to within  $\pm 30\%$ . However, the RMS error is 35%, but the mean error is -17%.

Two-phase flow on the shell side of a shell and tube heat exchanger is a complex flow. This study provides further understanding of the pressure drop phenomena that can occur. Further study involving other tube bundle arrangements and other fluids is therefore warranted.

## ACKNOWLEDGEMENT

The authors would like to thank the Universiti Tun Hussien Onn Malaysia (UTHM) and Ministry of Higher Education of Malaysia (MoHE) for financial support. This work was also supported by Research Acculturation Grant Scheme (RAGS) (No. R028).

## REFERENCES

- [1] Schrage, D. S., Hsu, J. T. and Jensen, M. K., Two-Phase Pressure Drop in Vertical Crossflow across a Horizontal Tube Bundle, *AICHE Journal*, Vol. 34(1), 1998, pp. 107-115.
- [2] Dowlati, R., Kawaji, M. and Chan, A. M. C., Pitch-to-Diameter Effect on Two-Phase Flow across an in-Line Tube Bundle, *AICHE Journal*, Vol. 36(5), 1990, pp. 765-772.
- [3] Feenstra, P. A., Weaver, D. S. and Judd, R. L., Improved Void Fraction Model for Two-Phase Cross-Flow in Horizontal Tube Bundles, *International Journal of Multiphase Flow*, Vol. 26(11), 2000, pp. 1851-1873.
- [4] Ishihara, K., Palen, J. W. and Taborek, J., Critical Review of Correlations for Predicting Two-Phase Flow Pressure Drop across Tube Banks, *Heat Transfer Engineering*, Vol. 1(3), 1980, pp. 23-32.
- [5] Xu G.P., Tso C.P., Tou K.W., Hydrodynamics of two-phase flow in vertical up and down-flow across a horizontal tube bundle, *International Journal of Multiphase Flow*, 24, 1998, 1317-1342.

- [6] McNeil D.A., Sadikin A., Bamardouf K.H., A mechanistic analysis of shell-side two-phase flow in an idealized in-line tube bundle, *International Journal of Multiphase Flow*, 45, 2012, 53-69.
- [7] Patrick M. Swanson B.S., Radiation attenuation method of measuring density of a two-phase fluid, *The Review of Scientific Instruments*, 29, 1958, 1079-1085.
- [8] Chisholm D., 1983. Two-phase flow in pipelines and heat exchangers. George Goodwin, London and New York.
- [9] Dowlati, R., Chan, A. M. C. and Kawaji, M., Hydrodynamics of Two-Phase Flow across Horizontal in-Line and Staggered Rod Bundles, *Journal of Fluids Engineering, Transactions of the ASME*, Vol. 114(3), 1992, pp. 450-456.
- [10] ESDU, Crossflow Pressure Loss over Banks of Plain Tubes in Square and Triangular Arrays Including Effects of Flow Direction, *Engineering Sciences Data Unit*, Vol.(79034), 1979, pp. 17.